Open Access Journal

Journal of Power Technologies 98 (1) (2018) 106–120

journal homepage:papers.itc.pw.edu.pl

Coordinated design of PSS and TCSC based on Fuzzy controller using global signals

Ali Ghasemi[a,*], Hossein Shayeghi[a]

[a] *Technical Engineering Department, University of Mohaghegh Ardabili, Ardabil, Iran*

Abstract

This paper presents a modified chaotic gravitational search algorithm (CGSA) as a novel heuristic algorithm for coordinate design of fuzzy logic controller-based thyristor controlled series capacitor (FLC-TCSC) and power system stabilizers (PSSs) in multi-machine power system. The coordinate design of PSS and FLC-TCSC damping controllers is converted to a single optimization problem with the time-domain objective function which is solved by the proposed CGSA algorithm which has strong ability for finding the most optimistic results. By minimizing the employed fitness function in which oscillatory characteristics between areas are included, the interactions among the FLC-TCSC controller and PSS under transient conditions in the multi-machine power system are enhanced. The generator speed and the electrical power are chosen as global input signals. The system performance is assessed through the time multiplied absolute value of the error (ITAE), Eigenvalues and figure of demerit (FD) analysis performance indices. The robustness is tested by considering several operating conditions to establish the superior performance with the proposed controller over the other stabilizers.

Keywords: Small signal stability, gravitational search algorithm, multi-machine system, fuzzy controller, FACTs devices, optimization.

1. Introduction

1.1. Aims and difficulties

Power systems are complex multi-component dynamic systems in which the system characteristics are used to fluctuate with varying loads and varying generation schedules. These power systems suffer by low frequency oscillations on sudden changes in load or occurrence of fault. The transfer of bulk power across weak transmission lines is hindered due to continuous persistence of such a low-frequency oscillation (0.2 .. 3.0 Hz) [1]. To improve the small signal instabilities caused by the automatic voltage regulator (AVR) and other factors, PSS was introduced to stabilize the system and increase the system's security [2]. With speed or frequency used as PSS inputs, a torsional filter is also commonly used. The PSS design problem therefore calls for coordinating the parameters of the different stabilizers so that the damping of the system's electromechanical modes is increased. An important issue in the design of controllers is robustness, i.e., the controller should achieve the desired damping over a wide range of system operating conditions. However, during some operating conditions, these devices may not produce adequate damping, and other effective alternatives are needed in addition to PSS. Recent development of power electronics introduces the use of flexible AC transmission system (FACTS) controllers in power systems. FACTS controllers are capable of controlling the network condition in a very fast manner and this feature of FACTS can be exploited to improve the stability of a power system [3–5]. TCSC is one of the important members of FACTS family which can be installed in series in the transmission lines. The interaction among PSSs and TCSC-based fuzzy controller may enhance or degrade the damping of certain modes of rotor's oscillating modes.

1.2. Literature review

In [6] proposed the steady state impedance pattern of the TCSC compensator installed at the Kayenta substation and USA. The effect of sub-synchronous resonance (SSR) for mentioned substations presented in [7]. The TCSC current regulator mode is used to assess the impact on the shaft torque during three phase faults. It was observed that the shaft torque with the TCSC compensated system were essentially the same as the torque found for uncompensated system. In [8] analyzed the performance of TCSC for SSR. They considered a radial transmission system and focused on destabilization of a particular torsional mode when minor disturbance takes place. It was shown that with TCSC,

*Corresponding author
Email address: ghasemi.agm@gmail.com (Ali Ghasemi)

damping of the particular mode is significantly improved. In [9], a coordinated design for single machine infinite bus (SMIB) based on excitation system and unified power flow controller (UPFC) controller by using the feedback linearization theory is proposed. This method is also used for designing thyristor controlled phase shifting (TCPS) [10], static var compensator (SVC) [11] and shunt static synchronous compensators (STATCOM) [12] controllers with excitation system, simultaneously. In [13] back-stepping method is used to design TCSC controller and excitation system coordinately. It is shown that it can improve the transient stability, the system damping and the voltage regulation. The application of FACTs for power oscillation damping, stability enhancement and frequency stabilization can be found in several references [14–17]. These methods can be classified into two models; nonlinear and linear. On the other hand, linear model cannot properly tackle the complex dynamics of the system, especially during the critical faults. Moreover, recently, several heuristic methods have been developed for robust tuning of PSS and FATCs such as particle swarm optimization (PSO) [18], simulated annealing (SA) [19], real code genetic algorithm (RCGA) [20] and artificial neural network (ANN) [21]. In [22], proposed robust H∞ theory to provide control signals toward enhancing the system damping of low frequency oscillations associated and guarantee non degradation of torsional phenomenon by considering the high frequency un-modeled dynamics in the power system. In [21] ANN has been suggested for FACTs design based on two reasons. First, since ANN is based on parallel processing, it can supply fast processing facility. Next reason is its ability to realize nonlinear mapping pattern between the input- and output-space. These heuristic methods have many disadvantages associated with them such as insecure convergence, disadvantages associated with the piecewise quadratic cost approximation and may even fail to converge due to in appropriate initial conditions when the system has a highly epistatic objective function (i.e. where parameters being optimized are highly correlated), and number of variables to be optimized is large [23–26]. In other hands, many researchers has applied the gravitational search algorithm on large numbers of problems because it requires only two parameters and having ability to find near global optimum solution and provides better results as compare to other nature inspired algorithms.

1.3. Motivations and contributions

The main contributions of this paper are as follows:

1. This paper investigates the application of TCSC hybrid controller for improving damping inter-area modes of oscillations. The major advantage of the proposed FLC based on TCSC stabilizer is its model independency.
2. Selection of the best input signal problem is one of the most issues in control theory. In this paper FLC-TCSC has been applied with two global input signals, namely, electrical power (Pe) and machine speed (ω). Therefore, the developed FLC model with more fuzzy inference rules has been applied through which a flexible control of reactance (X_{TCSC}). In addition, this paper presents a new model of finding the best membership functions in fuzzification process.
3. To avoid the disadvantage of traditional method for finding the global optimum solution and ensure the final solution is not a local optimal solution, a new modified of gravitational search algorithm (GSA) based chaos local search (CLS), namely CGSA is proposed for finding the optimal parameters of FLC-TCSC and PSS stabilizers.

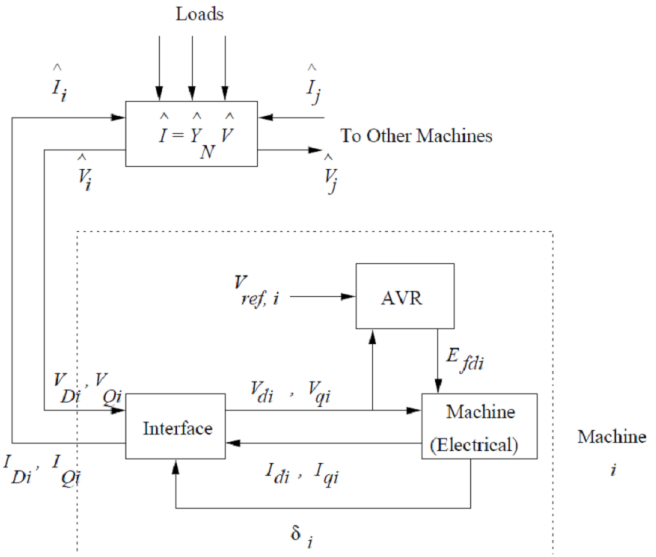

Figure 1: Structure of a multimachine system

2. Power System Formulation

Figure 1 shows the schematic of a multimachine system. This section describes the dynamic equations represented by each block shown in the ith machine and external network. It is assumed that power system consists of n number of generators and generators feed local loads which are constant [1].

2.1. Non-linear model

A number of analytic models with the same differential-algebraic structure are given in [1, 2]. One of them is a simple non-linear multi-machine model, which makes it possible to analytically investigate the impact of controlled active power on electromechanical dynamics. The system dynamics of the synchronous machine can be expressed as a set of five first order linear differential equations given in equations (1) – (5) [5].

$$\dot{\delta}_i = \omega_b(\omega_i - 1) \tag{1}$$

$$\dot{\omega}_i = \frac{1}{M_i}(P_{mi} - P_{ei} - D_i(\omega_i - 1)) \tag{2}$$

$$\dot{E}'_{qi} = \frac{1}{T'_{doi}}(E_{fdi} - (x_{di} - x'_{di})i_{di} - E'_{qi}) \tag{3}$$

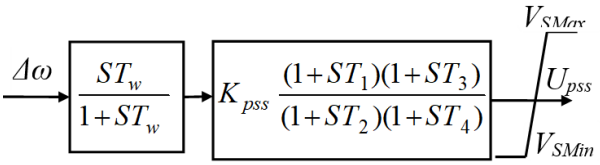

Figure 2: Structure of power system stabilizer

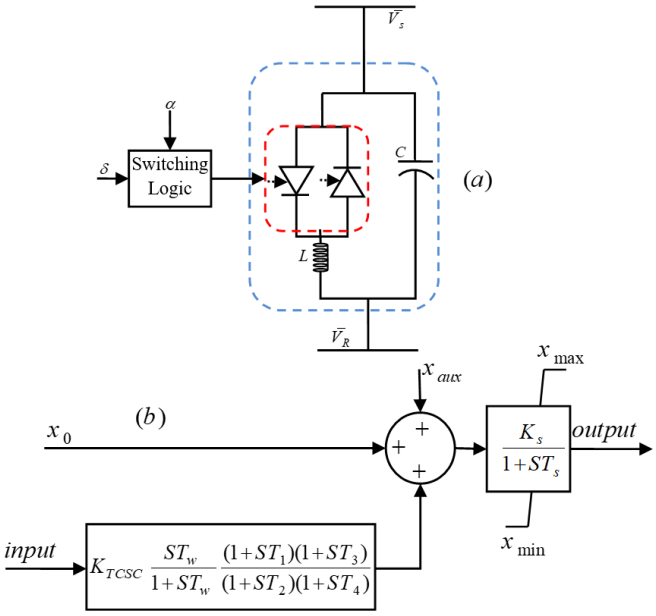

Figure 3: TCSC dynamic model (a) TCSC model and (b) structure of TCSC based controller

$$\dot{E}_{fdi} = \frac{1}{T_{Ai}}(K_{Ai}(v_{refi} - v_i + u_i) - E_{fdi}) \tag{4}$$

$$T_{ei} = E'_{qi} i_{qi} - (x_{qi} - x'_{di})\, i_{di}\, i_{qi} \tag{5}$$

where, i_d and i_q are d-q components of armature current. E_{fd}, E'_d and E'_q are voltage proportional to field voltage, damper winding flux and field flux, respectively. Also, T'_{d0} and T'_{q0} are d-axis and q-axis transient time constant, respectively.

2.2. PSS structure

The main objective of the PSS is to provide additional damping in order to stabilize an oscillatory unstable system. PSS controller design, methods of combining the PSS with the AVR, investigation of many different input signals and the vast field of tuning methodologies are all part of the PSS topic. The PSS usually uses shaft speed, active power output or bus frequency as input. The stabilizer itself mainly consists of two lead-lag filters as shown in Fig. 2.

The PSS parameters to be optimized are the time constants T_1,..., T_4 and gain K_{pss}. T_w is 10 seconds and is constant for all machines in other to ensure that the phase-lead and gain contributed by the washout block for the range of oscillation frequencies normally encountered is negligible [1].

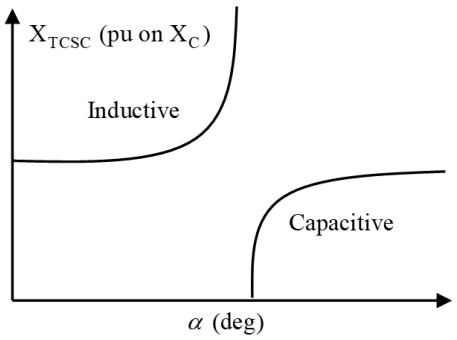

Figure 4: Variation of the TCSC reactance with firing angle α

2.3. Modeling and control of TCSC

The TCSC is a device placed on transmission lines rather than being connected in shunt at a single power system bus, e.g., SVC. The series connection scheme allows the power flow to be influenced through changing the effective admittance linking two buses, and is a method of improving transient stability limits and increasing transfer capabilities [27]. TCSC model and its damping controller [28] are shown in Fig. 3(a)-(b), respectively. They shows concept of a variable series reactance which is adjusted through appropriate variation of the firing angle (α). As shown in Fig. 3(b), this controller may be considered as a lead-lag compensator. It comprises gain block, signal-washout block and two stages of lead-lag compensator. Neglecting washout stage, the TCSC controller can be represented by the following state equations;

$$\begin{cases} \Delta\dot{\alpha} = -\frac{1}{T_2}\Delta\alpha - \frac{K_{TCSC}}{\omega_s}(\frac{1}{T_2})\Delta\omega - \frac{K_{TCSC}}{\omega_s}(\frac{T_1}{T_2})\Delta\dot{\omega} \\ \Delta\dot{x}_{TCSC} = -\frac{1}{T_{TCSC}}(\Delta\alpha - \Delta x_{TCSC}) \end{cases} \tag{6}$$

The steady-state formulation based α and X_{TCSC} is shown [29]:

$$\begin{gathered} x_{TCSC} = -x_C - C_1(2(\pi-\alpha) + \sin(2(\pi-\alpha))) + \\ -C_2\cos^2(\pi-\alpha) \times (\bar{\omega}\tan(\bar{\omega}(\pi-\alpha)) - \tan(\pi-\alpha)) \\ x_{LC} = \frac{x_L x_C}{x_C - x_L}, C_1 = \frac{x_C + x_{LC}}{\pi}, C_2 = \frac{4x_{LC}^2}{\pi x_L} \end{gathered} \tag{7}$$

The TCSC linearized equivalent reactance, which can then be obtained from Eq. (8), is:

$$\begin{gathered} \Delta x_{TCSC} = \{-2C_1(1+\cos(2\alpha)) + C_2\sin(2\alpha)(\bar{\omega}\tan(\bar{\omega}(\pi-\alpha)) + \\ -\tan(\alpha) + C_2(\bar{\omega}^2\frac{\cos^2(\pi-\alpha)}{\cos^2(\bar{\omega}(\pi-\alpha))} - 1)\}\Delta\alpha \end{gathered} \tag{8}$$

For a TCSC designed with $X_C = 5.75X_L$ Ω at a base frequency of 50 Hz, its equivalent reactance (XTCSC) as a function of the firing angle (α) has been plotted in Fig. 4.

2.4. Fuzzy logic-based damping controller design

The proposed fuzzy logic-based TCSC damping strategy with two global signals$\Delta\omega$ and ΔP_e is shown in Fig. 5. Figure 6 depicts the employed membership functions. The two inputs and one output control signal are represented by seven triangular membership functions in fuzzy variable space [12]. These membership functions are described by linguistic terms, Negative Big (NB), Negative Medium (NM),

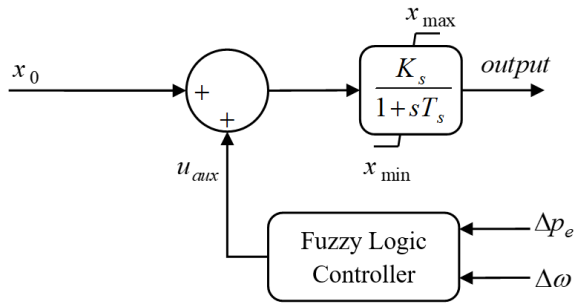

Figure 5: Block diagram of proposed fuzzy logic control

Negative Small (NS), Zero (ZE), Positive Small (PS), Positive Medium (PM) and Positive Big (PB) for$\Delta\omega$ and ΔP . The membership functions for the output control signal are described by Output Negative Big (ONB), Output Negative Medium (ONM), Output Negative Small (ONS), Output Zero (OZE), Output Positive Small (OPS), Output Positive Medium (OPM) and Output Positive Big (OPB). The table of fuzzy rules which is extracted from experience and engineering knowledge, for two inputs and the sole output are given in [12]. With seven membership functions for two inputs, 25 rules can be introduced for fuzzy controller design.

3. Chaotic Gravitational Search Algorithm

3.1. Overview GSA

GSA was proposed by E. Rashedi et al in 2009 [30]. It is a new heuristic algorithm that has been acceptable performance in the optimization problems. One of the major benefits is its capability to find the global optimum in a shorter time compare to other heuristic algorithms, which it works based on gravity rules. It likes a small artificial world of masses obeying the Newtonian laws of gravitation and motion such as:

- Law of gravity: each agent attracts every other agent and the gravitational force among two agents is directly proportional to the product of their masses and inversely proportional to the square of the distance among them.
- Law of motion: The present velocity of any mass is equal to the sum of the fraction of its earlier velocity and the variation in the velocity. Variation in the acceleration/velocity of any mass is equal to the force acted on the system divided by mass of inertia.

To explain the GSA, consider a system with s agents (masses) in which position of the i^{th} mass is given by:

$$X_i = (x_i^1, ..., x_i^d, ..., x_i^n), i = 1, 2, ..., s \tag{9}$$

where, $x_i^d$is position of the i^{th} mass in the d^{th} dimension of n-dimension. Pursuant to [30], mass of each agent is obtained after calculating current agent's fitness as follows:

$$M_i(t) = \frac{q_i(t)}{\sum_{j=1}^{s} q_i(t)} \tag{10}$$

where, $M_i(t)$ and $q_i(t)$ are the mass value of the i^{th} agent at time t and the gravitational masse which is updated by:

$$q_i(t) = \frac{fit_i(t) - worst(t)}{best(t) - worst(t)} \tag{11}$$

where, $fit_i(t)$, $worst(t)$ and $best(t)$ are the fitness value of the i^{th} agent at time t, worst and best fitness value which defined by:

$$\begin{cases} worst(t) = Max_{j\in\{1,...,s\}} fit_i(t) \\ best(t) = Min_{j\in\{1,...,s\}} fit_i(t) \end{cases} \tag{12}$$

To calculate acceleration of the agent i, total forces $F_i^d(t)$ from a set of heavier masses that apply on this agent should be considered based on the law of gravity, which is followed by computation of agent acceleration $a_i^d(t)$:

$$F_i^d(t) = \sum_{j\in kbest, j\neq i} rand_i G(t) \frac{M_j(t)M_i(t)}{R_{ij}(t) + \varepsilon}(x_j^d(t) - x_i^d(t)) \tag{13}$$

$$a_i^d(t) = \frac{F_i^d(t)}{M_i(t)} = \sum_{j\in kbest, j\neq i} rand_j G(t) \frac{M_j(t)}{R_{ij}(t) + \varepsilon}(x_j^d(t) - x_i^d(t)) \tag{14}$$

Thenceforth, next velocity of the agent is computed as a part of its existing velocity added to its acceleration that defined as:

$$V_i^d(t+1) = rand_i \times v_i^d(t) + a_i^d(t) \tag{15}$$

Then, the agent position can be updated by:

$$x_i^d(t+1) = x_i^d(t) + v_i^d(t+1) \tag{16}$$

where, $rand_i$ and $rand_j$ are two uniformly distributed random numbers in the interval [0, 1], $R_{ij}(t)$ is the Euclidean distance between two agents i and j that calculated by $R_{ij}(t) = \|X_i(t), X_j(t)\|_2$, ε is a small value, k_{best} is the set of first K agents with the best fitness value and biggest mass, which become a function of time with the initial value K_0 at the beginning and decreasing with time. Here, K_0 is set to the total number of agent's s and is eliminated linearly to 1. G shows the gravitational constant, initialized to G_0, and updated with time:

$$G(t) = G(G_0, t) \tag{17}$$

For better perception see Fig. 7. The GSA has some differences and advantages compared to other heuristic algorithms [1]:

- The agent direction is computed based on the general force given by all other agents.
- The force has direct comparative to fitness value and so updating procedure is performed considering fitness value of the solutions.
- It is memory-less and only current agent plays a role in the updating process.
- In updating process, the force is inversely proportional to the distance between solutions.

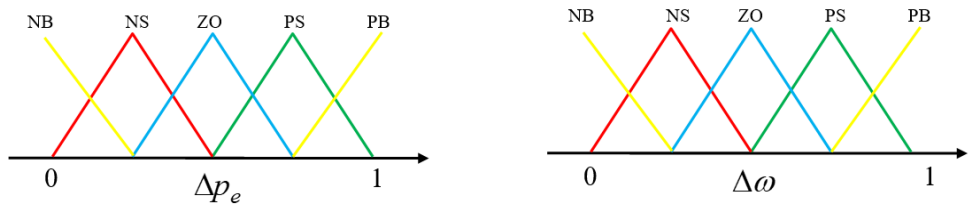

Figure 6: Fuzzy membership functions for global signals

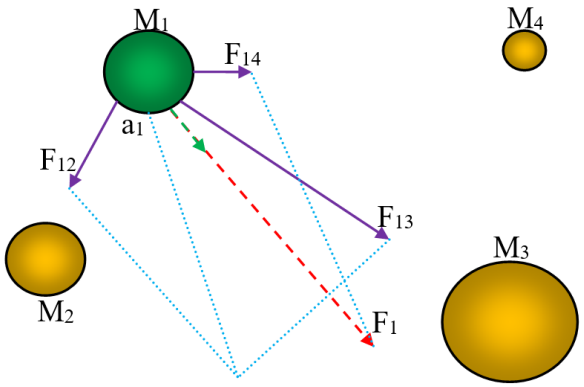

Figure 7: Graphical structure for GSA

3.2. Chaotic GSA

To achieved a good decision for simulating complex phenomena, sampling, numerical analysis in heuristic optimization needs random sequences with a long period and good uniformity. Chaos is a deterministic, random like process found in dynamical system, non-linear, which is non-converging, non-period and bounded. GSA method has gained much attention and widespread applications in different optimization fields. But, it often converges to local optima. In order to overcome this shortcoming, we propose CGSA method that combines GSA with chaotic local search (CLS). There are two CLS procedures. In the first CLS method, CLS is based on the Tent equation (CLS_1) [31], while the latter CLS (our proposed) is based on the forcing the pendulum (CLS_2). In other words, we see that the instability of the specified motions is exactly what should make them helpful. Assume that our array of sensors controls the current C_{i+1}^j that is formulated based forcing of the pendulum, by rewritten it from $cos(t)$ to something like:

$$c_{i+1}^j = \begin{cases} 2c_i^j, if\ 0 < c_i^j \le 0.5 \\ 2(1-c_i^j), if\ 0.5 < c_i^j \le 1 \end{cases}, \ j = 1, 2, ..., Ng, \{Tend\} \tag{18}$$

$$c_{i+1}^j = \begin{cases} 2c_i^j \times (1+\frac{g_{best}^{k-1}}{g_{best}^k}) \times cos(2\pi \frac{g_{best}^{k-1}}{g_{best}^k}), \ 0.5 < c_i^j \le 1 \\ 0.1c_i^j \times (1 - cos((1+\frac{g_{best}^{k-1}}{g_{best}^k}))), \ 0 < c_i^j \le 0.5 \end{cases} \{proposed\ method\} \tag{19}$$

where, g_{best}^k is best optimal value for k^{it} iteration and $\frac{g_{best}^{k-1}}{g_{best}^k}$ represents the fine tuning necessary to achieve the desired sequence of gyrations. The chaotic local search on the GSA algorithm can be summarized as follows:

Step 1: Generate an initial chaos population randomly for CLS

$$\begin{aligned} X_{cls}^0 &= [X_{cls,0}^1, X_{cls,0}^2, ..., X_{cls,0}^{Ng}]_{1\times N_g} \\ cx_0 &= [cx_0^1, cx_0^2, ..., cx_0^{Ng}] \\ cx_0^j &= \frac{X_{cls,0}^j - P_{j,\min}}{P_{j,\max} - P_{j,\min}}, \ j = 1, 2, ..., Ng \end{aligned} \tag{20}$$

where, the chaos variable can be generating as follows:

$$\begin{aligned} X_{cls}^i &= [X_{cls,i}^1, X_{cls,i}^2, ..., X_{cls,i}^{Ng}]_{1\times N_g}, i = 1, 2, ..., N_{chaos} \\ x_{cls,i}^j &= cx_{i-1}^j \times (P_{j,\max} - P_{j,\min}) + P_{j,\min}, j = 1, 2, ..., N_g \end{aligned} \tag{21}$$

Step 2: Determine the chaotic variables

$$\begin{aligned} cx_i &= [cx_i^1, cx_i^2, ..., cx_i^{Ng}], \ i = 0, 1, 2, ..., N_{choas} \\ cx_{i+1}^j &= baseCLS, \ j = 1, 2, ..., Ng \\ cx_0^j &= rand(0) \end{aligned} \tag{22}$$

where, N_{chaos} is the number of individuals for CLS. Cx_i^{Ng} is thei^{th} chaotic variable. $Rand()$ generate a random number between 0 and 1.
Step 3: Mapping the decision variables.
Step 4: Convert the chaotic variables to the decision variables.
Step 5: Evaluate the new solution with decision variables.

4. Applied of CGSA for proposed strategy

A proposed problem is formulated to optimize a composite set of objective function comprising the damping factor, and the damping ratio of the lightly damped electromechanical modes, and the effectiveness of the suggested technique is confirmed through eigenvalue analysis and nonlinear simulation results. The simulation operated with single objective with CGSA algorithm and the objective functions for optimization as follow:

$$ISTSE = \sum_{j=1}^{N_p} \sum_{i=1}^{N_g} \int_0^{t_{sim}} t^2.(|\Delta\omega_{ij}|^2).dt \tag{23}$$

where, N_P, N_g and t_{sim} are number of operating condition, number of generators and the time of simulation, respectively. The optimal proposed controller tuning parameters problem can be formulated as the following constrained optimization problem, where the constraints are the PSS parameters bounds [1]. The optimization Problem can be stated as:

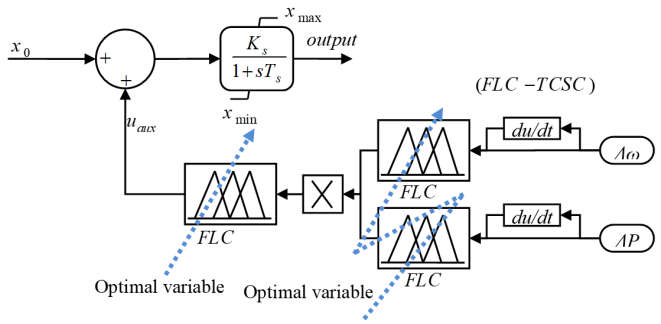

Figure 8: The proposed FLC

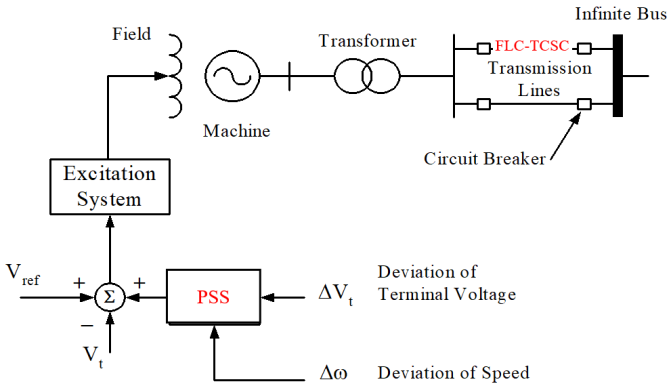

Figure 9: Schematic diagram of single machine infinite bus system

$$\begin{aligned} &Minimize\ J\ Subject\ to: \\ &K^{\min} \le K \le K^{\max} \\ &T_1^{\min} \le T_1 \le T_1^{\max} \\ &T_3^{\min} \le T_3 \le T_3^{\max} \end{aligned} \tag{24}$$

Typical ranges of the optimized parameters are [0.01-50] for Kpss and [0.01-1] for T_1,T_3. The PSS parameters (T_2, T_4, and T_w) are considered fixes; their values are 0.02, 0.02 and 10, respectively. The graphical model of the proposed technique is shown in Fig. 8. In this study, in order to acquire better performance, agent dimension, population size, G_0 and α are chosen as number of dimension, 40, 60, 20 and 100, respectively. It should be noted that CGSA technique is run several times and then optimal set of proposed controller problem is selected.

The performance of power systems equipped with PSS and FLC-TCSC is validated for single machine infinite bus (SMIB) Fig. 9 and the four-machine two-area study system Fig. 10. Based on Fig. 10 each area contains some part with characteristic that generator with 900 MVA and 20 kV. Each of the units is connected through transformers to the 230 kV transmission line. There is a power transfer of 400MW from area 1 to area 2. The detailed bus data, line data, and the dynamic characteristics for the machines, exciters and loads are given in APPENDIX.

Different operating conditions are analyzed for the SMIB and TAFM power system, as given in Tables 1 and 2, respectively. The optimum variables parameters are given in Tables 3 and 4 for SMIB and TAFM power system, respectively.

Table 1: Operating conditions (SMIB)

Case No.	P	Q	x_e	H
Case1 (Base case)	0.8	0.4	0.3	3.25
Case 2	0.5	0.1	0.3	3.25
Case 3	1	0.5	0.3	3.25
Case 4	0.8	0.4	0.6	3.25
Case 5	0.5	0.1	0.6	3.25
Case 6	1	0.5	0.6	3.25
Case 7	0.8	0	0.6	3.25
Case 8	1	-0.2	0.3	3.25
Case 9	0.5	-0.2	0.6	3.25
Case 10	1	-0.2	0.3	0.81

Fig. 11 show the minimum fitness functions evaluating process.

To demonstrate performance robustness of the proposed method, two performance indices: the Integral of the Time multiplied Absolute value of the Error (ITAE) and Figure of Demerit (FD) based on the system performance characteristics are defined as

$$ITAE = 10 \times \sum_{i=1}^{N_G} \int_0^{t_{sim}} t.(|\Delta\omega_i|).dt \tag{25}$$

$$FD = \frac{\sum_{i=1}^{N_G}((500 \times OS_i)^2 + (8000 \times US_i)^2 + 0.01 \times T_{s,i}^2)}{N_G} \tag{26}$$

where, Overshoot (OS), Undershoot (US) and settling time of rotor angle deviation of machine is considered for evaluation of the FD. It is worth mentioning that the lower value of these indices is, the better the system response in terms of time domain characteristics.

5. Simulation and Discussion

5.1. SMIIB Power System

The behavior of the proposed algorithm based coordinate designed FLC-TCSC and PSS under transient conditions is verified by applying disturbance and fault clearing sequence under different operating conditions in comparison with the PSO based tuned PSS (PSOPSS) [32] and classical PSS [33]. The disturbances are given at t = 1 sec. System responses in the form of slip (Sm) are plotted. The following types of disturbances have been considered.

Scenario 1: A step change of 0.1 pu in the input mechanical torque.

Scenario 2: A three phase-to-ground fault for 100 ms at the generator terminal.

Figure 12 shows the system response at the lagging power factor operating conditions with weak transmission system for scenario 1. It can be seen that the system with CPSS is highly oscillatory. Both proposed controller and PSOPSS are able to damp the oscillations reasonably well and stabilize the system at all operating conditions. System response at the ohmic operating conditions is shown in Fig. 13 with the weak and strong transmission system for scenario 1. The proposed technique is effective and achieves good system

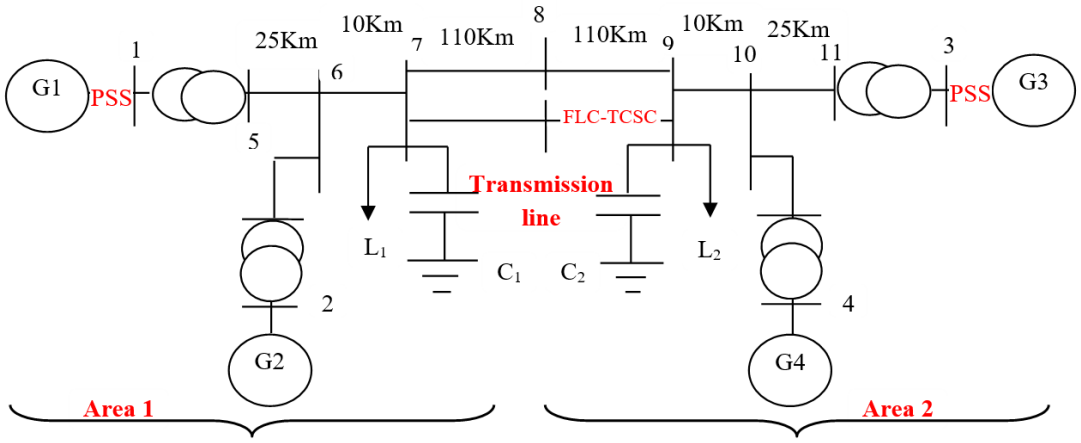

Figure 10: Two-Area Four-Machine (TAFM) power system

Table 2: Operating conditions (TAFM)

Conditions NO	G1		G2		G3		G4	
	P	Q	P	Q	P	Q	P	Q
1	0.7778	0.1021	0.7777	0.1308	0.7879	0.0913	0.7778	0.0918
2	1.084	0.3310	0.7778	0.4492	0.7879	0.1561	0.7778	0.2501
3	0.7778	0.0502	0.2333	0.0371	0.7989	0.0794	0.7778	0.0704
4	0.7778	0.1021	0.7777	0.1308	0.7989	0.0903	0.7778	0.0981
Other Characteristics								
5	20% increase load							
6	20% decrease load							
7	2 line tripe: 7-8, 8,9							

Table 3: Optimal parameters (SMIB)

PSS					$TCSC$						
K_{pss}	T_1	T_2	T_3	T_4	K_{TCSC}	T_1	T_2	T_3	T_4	V_{max}	V_{min}
12.5	0.073	0.028	3	5.4	18.32	0.873	0.253	0.984	0.056	0.113	-0.129

Table 4: Optimal parameters (TAFM)

Model	PSS					$TCSC$				
Gen	K_{pss}	T_1	T_2	T_3	T_4	K_{TCSC}	T_1	T_2	T_3	T_4
G_1	22.87	2.12	1.17	6.09	7.43	20.827	0.748	0.184	0.694	0.084
G_3	19.32	2.02	1.21	4.82	6.32					

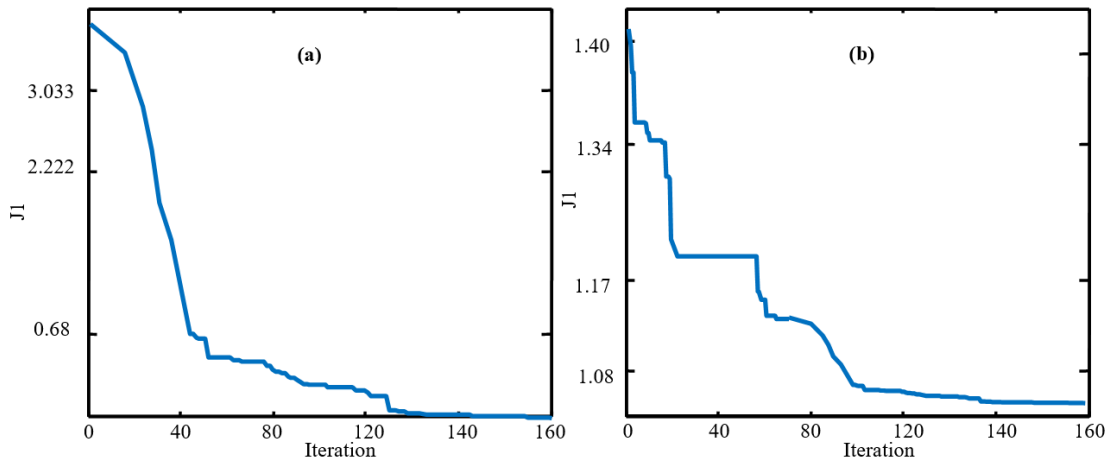

Figure 11: Fitness convergence with proposed algorithm (a) (SMIB), (b) (FLC-TCSC)

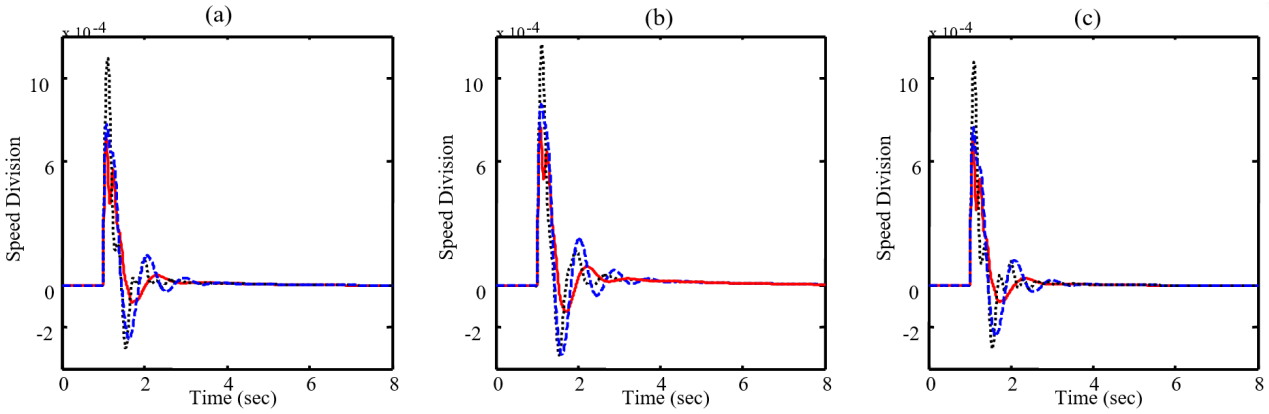

Figure 12: ΔTm=0.1 (p.u.) under Xe=0.3; CPSS (Dotted), PSOPSS (Dashed) and Our Method (Solid) a) P=0.8, Q=0.4 b) P=0.5, Q=0.1 c) P=1.0, Q=0.5

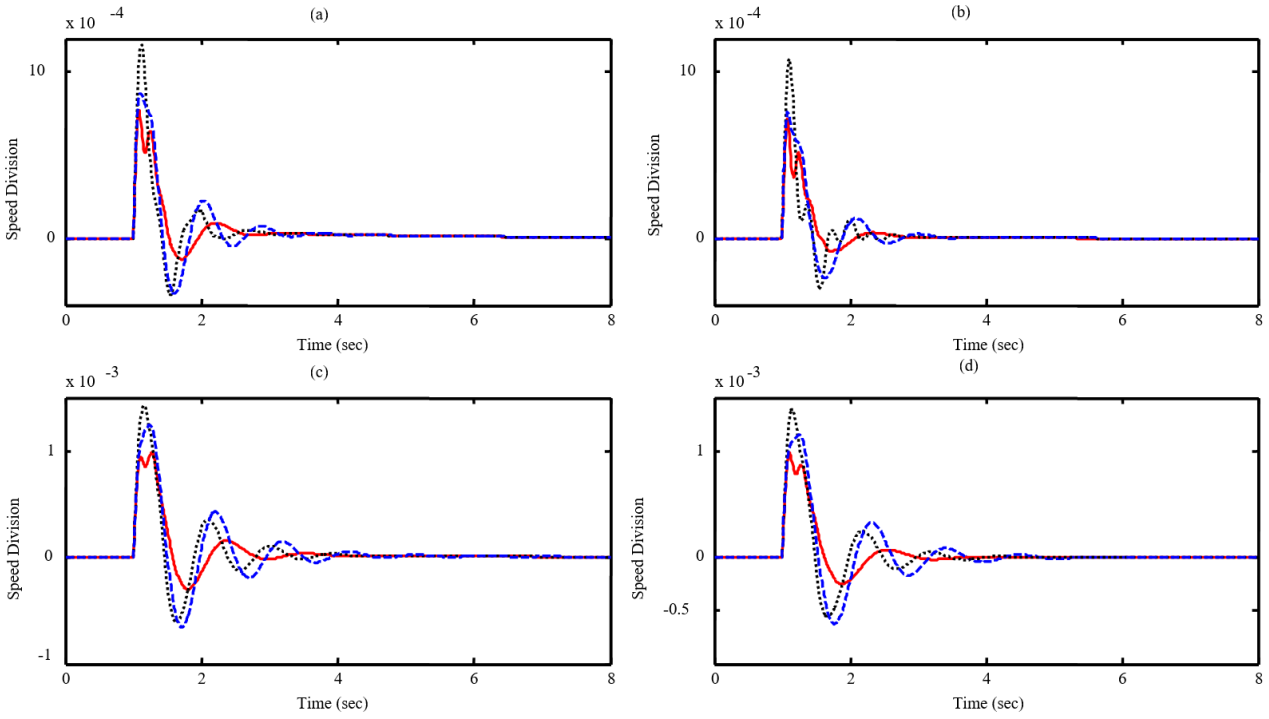

Figure 13: ΔTm=0.1 (p.u.); CPSS (Dotted), PSOPSS (Dashed) and Our Method (Solid) Xe=0.3; a) P=0.5, Q=0.0 b) P=1.0, Q=0 Xe=0.6; c) P=0.5, Q=0.0 d) P=1.0, Q=0

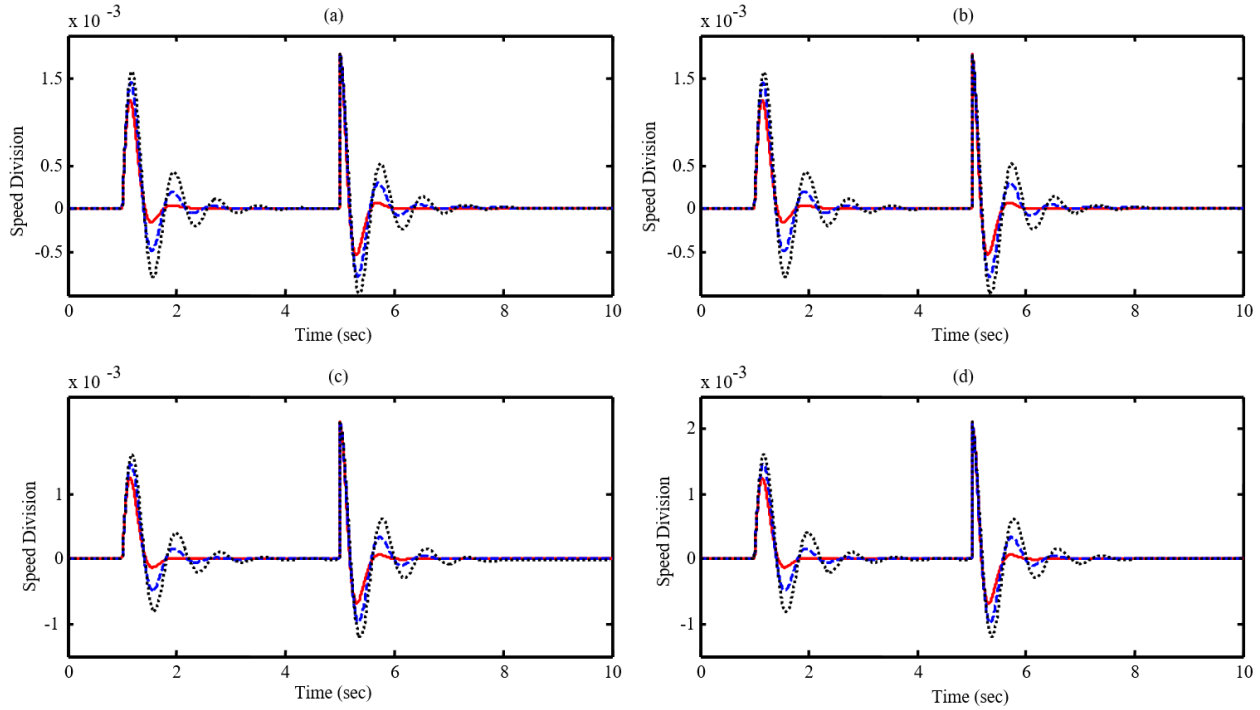

Figure 14: System response in scenario 3; CPSS (dotted), PSO (dashed-dotted) and our Method (solid) (a) P=0.8, Q=-0.2, Xe=0.3 (b) P=0.8, Q=0.0, Xe=0.6 (c) P=1.0, Q=-0.2, Xe=0.3 (d) P=1.0, Q=0.2, Xe=0.6 and $H' = H/4$

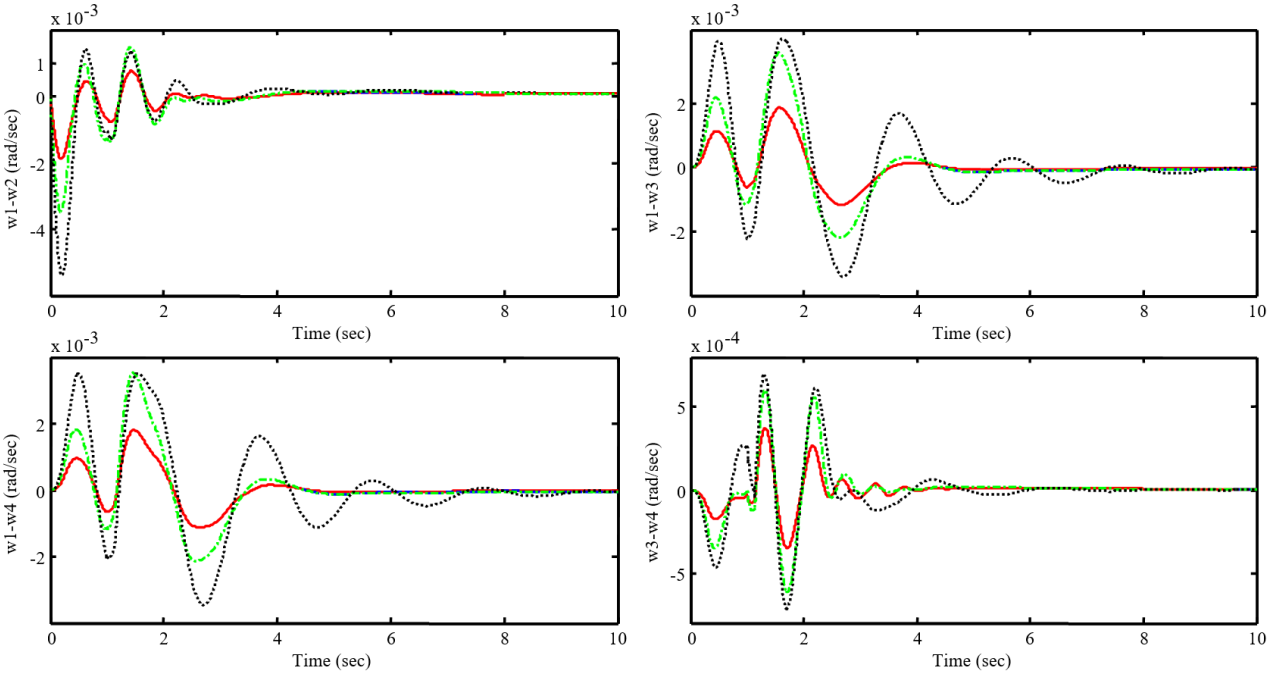

Figure 15: TAFM system response under nominal condition in scenario I; Solid (our Method) Dash-dotted (BFA [34]) and dot (CPSS [33])

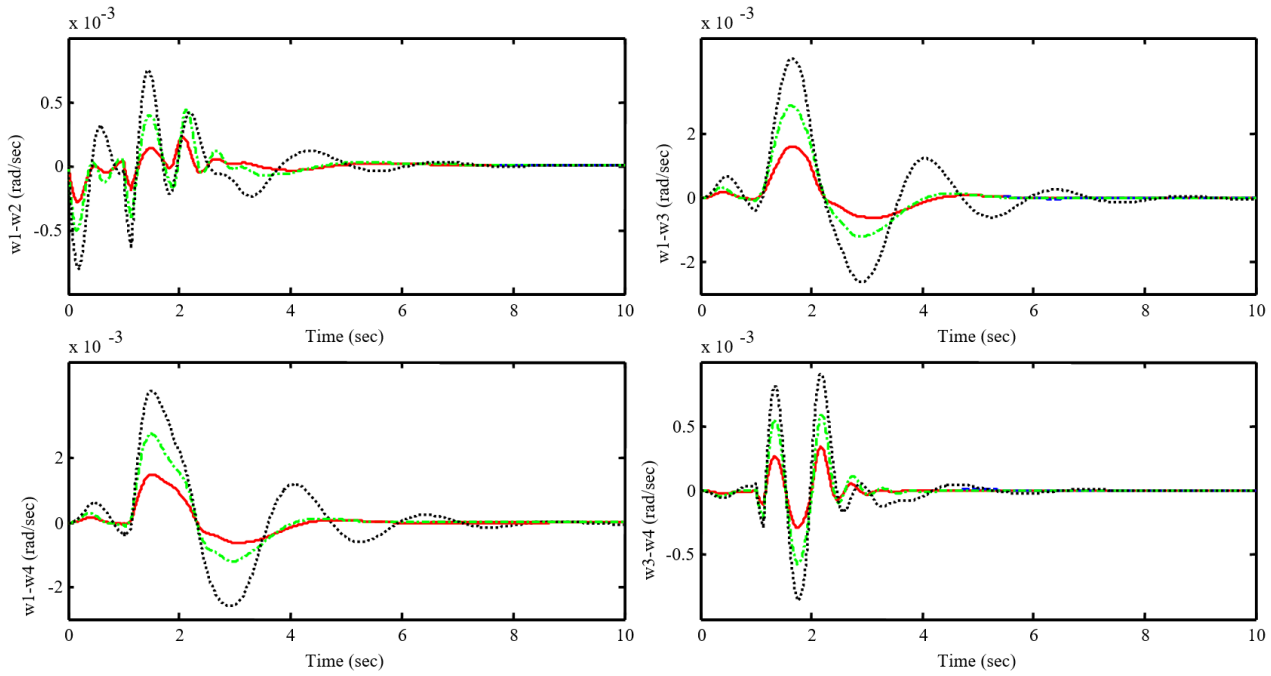

Figure 16: TAFM system response under heavy condition in scenario I; Solid (our Method) Dash-dotted (BFA [34]) and dot (CPSS [33])

damping characteristics. Figure 14 depicts the system response in scenario 1 with inertia $H' = H/4$. It can be seen that the proposed CGSA based coordinated PSS and FLC-TCSC has good performance in damping low frequency oscillations and stabilizes the system quickly. Moreover, it is superior to the PSOPSS and classical based methods tuned stabilizer.

5.2. TAFM Power System

5.2.1. Scenario 1

In this scenario, the performance of the proposed method tuning under transient conditions is verified by applying a 6-cycle three-phase fault at bus 7 at the end of line 7#8. The fault is cleared by permanent tripping of the faulted line. Figures 15 and 16 shows inter-area and local mode of oscillations response of generators 1, 2, 3 and 4 to the proposed fault, under normal and heavy operating condition. Numerical results of performance robustness for all system loading cases are shown in Fig. 17 with four stabilizers under scenarios 1. Assessment of these figures reveals that the using the proposed technique the speed deviations of all machines are greatly reduced, has small overshoot, undershoot and settling time. The electromechanical mode eigenvalues and the corresponding damping ratios for all methods are given in Table 5.

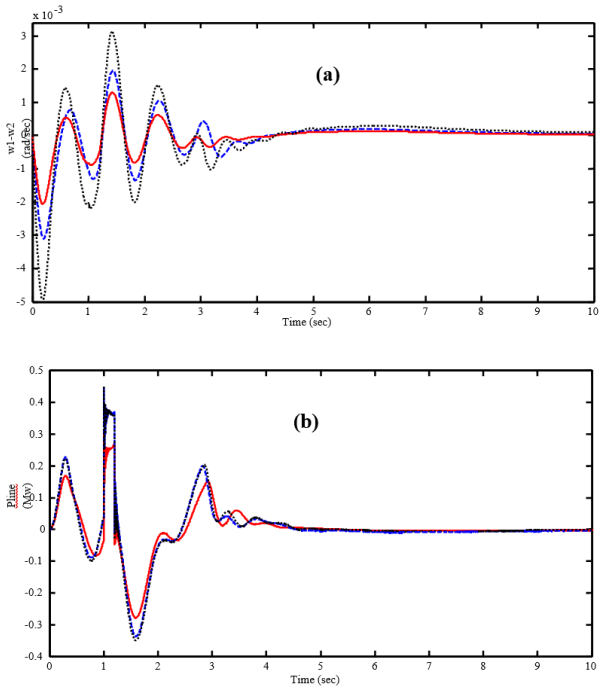

Figure 22: TAFM results: (a) rotor speed deviation of G_1-G_2; (b) transmitting power from area 1 to area 2. Solid (Proposed Method), Dashed (Tend), Dotted (Logistic)

5.2.2. Scenario II

In this scenario, the performance of the proposed PSS tuning under transient conditions is verified by applying a 6-cycle three-phase fault at bus 7 at the end of line 7#8 without line tripping and the original system is restored upon the clearance of the fault. The system response is shown

Table 5: Eigenvalues and damping ratios for 4-machine in scenario I

Algorithm	Base Case	20% increase	20% decrease	2 line tripe
Proposed Method	-23.5872 ± 24.6431i -22.9023 ± 19.4532i -2.9542 ± 11.8657i -2.2913 ± 7.8654i -1.5242 ± 2.0553i -1.0293 ± 0.5902i	-25.9845 ± 36.864i -0.3421 ± 0.1524i -0.0001 ± 0.0163i -0.3421 ± 0.0853i -0.0982 ± 0.0443i	-23.9283 ± 28.8234i -23.849 ± 18.9845i -2.6754 ± 12.675i -2.5473 ± 0.4234i -0.8928 ± 2.0495i -1.6384 ± 0.4533i	-24.7485 ± 24.1827i -1.3562 ± 5.5643i -0.0495 ± 3.0934i -3.5434 ± 1.5434i
BFA	-23.2414 ± 24.6055i -23.5574 ± 19.3215i -3.0039 ± 10.6336i -2.8771 ± 9.8092i -1.5039 ± 2.3150i -1.3113 ± 0.0749i -0.1067 ± 0.0100i	-25.7144 ± 36.9883i -0.1883 ± 0.0366i -0.1131 ± 0.0992i -0.0625 ± 0.1026i -0.0001 ± 0.0160i	-23.3296 ± 28.6551i -23.0396 ± 18.8225i -2.3029 ± 10.9392i -2.1772 ± 9.0308i -1.0568 ± 3.0740i -0.1084 ± 0.0072i	-24.6727 ± 24.9665i -1.6604 ± 6.2922i -1.4210 ± 4.0643i -0.1171 ± 3.3336i -1.1823 ± 0.0214i -0.1086 ± 0.0068i
CPSC	-23.4737 ± 26.5428i -23.7251 ± 21.5709i -1.8288 ± 6.7761i -2.0803 ± 7.0262i -0.6058 ± 2.8890i -0.1791 ± 0.0001i	-25.7018 ± 36.6545i -0.2124 ± 0.1418i -0.1578 ± 0.1652i -0.0558 ± 0.0940i -0.0001 ± 0.0160i	-23.1625 ± 29.8344i -22.1940 ± 20.3773i -2.1483 ± 8.0420i -1.6434 ± 5.7595i -0.4138 ± 3.3225i	-24.5154 ± 25.4120i -0.4669 ± 6.2506i -0.9653 ± 5.2795i -1.1065 ± 5.3156i -0.2262 ± 3.3310i

in Figs. 18 and 19 for different cases. It can be seen that the proposed technique has good performance in damping of the low frequency oscillations and stabilizes the system quickly. Numerical results of the system performance for different loading conditions are shown in Fig. 20.

From the loading conditions given in Table 1, approximately 6 operating conditions were generated to test the performance of the proposed PSS for a wide range of operating conditions. It is obvious that the electromechanical mode eigenvalues have been shifted to the left in s-plane and the system damping with the proposed method is greatly improved and enhanced.

5.3. Robustness analyze

The numerical result shows the potential of optimization design for PSS and FLC-TCSC with a time domain objective functions. For performance evaluation and robustness analyze of the proposed design technique, the two-area four-machine test power system using proposed method based proposed chaotic theory, logistic theory and Tend equation have been performed and the system performance has been examined. The optimization matter obtained using proposed methods are compared in Fig. 21. It is obvious that proposed method has better converge. This figure shows that the electro-mechanical modes are close together, but there is a higher difference in the other oscillatory mode of some PSSs. Also, instability of the open-loop system is obvious.

To investigate the coordination performance of the PSSs and FLC-TCSC under fault conditions, some large disturbances have been applied to the systems. We considered 9-cycle three phase ground fault at bus 1 cleared without equipment. Variations of active power of a selected line and rotor speed deviation of a generator located close to the fault position are plotted against time for various PSSs and the faulty operating condition as shown in Fig. 22. All of these figures present large signal stability of the test systems. Also it seems that, in CGSA based proposed theory has a better performance in most of the cases. However, more tests are needed to show the differences of the Pareto fronts' members clearly in future works.

Table 6: Different methods results comparison for TAFM power system

Method	Minimum	Mean	Maximum
Proposed method	0.0842	1.092	2.743
Based tend	0.0983	2.543	3.625
Based logistic	0.0995	2.948	4.421

Optimization results using proposed methods are presented in Table 6. This Table show that the average objective function produced by this method is least compared to the other reported approaches. It only reveals its capability to reach global minima in a consistent manner. Hence, it can be concluded that the proposed method has the stronger ability to find the superior quality solution and its convergence characteristic is also better.

6. Conclusion

In this paper coordination scheme to improve the stability of a power system by optimal design of power system stabilizer and TCSC-based fuzzy controller is presented. The coordinated design problem of PSS and FLC-TCSC damping controllers over a wide range of operation conditions is converted to an optimization problem and solved by a new modified optimization algorithm which has a strong ability to find the most optimistic results. Results show the CGSA technique has been successfully introduced to obtain the optimum solution of PSS and FLC-TCSC. Performance evaluation of proposed PSSs on single and multi machine systems shows that robust fixed parameter stabilizers are indeed a viable solution to the problem of low frequency oscillations. Eigenvalue analysis and extensive simulation studies show that the proposed method provides the desired closed loop performance over the prespecified range of operating conditions. The system performance characteristics indices reveal that the simultaneous coordinated designing of the TCSC damping controller and the PSS demonstrates its superiority to both the uncoordinated designed stabilizers of the PSS

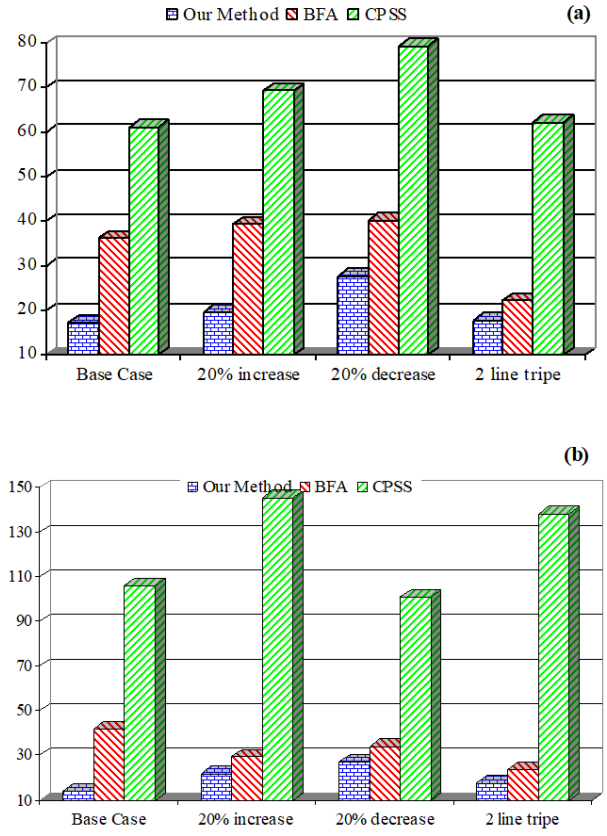

Figure 17: Values of performance index in scenario I; (a) ITAE and (b) FD

and the TCSC damping controller at large disturbance. The results show that the proposed technique has superior small signal stability. The important advantage of this proposed technique is that it can capture the complex dynamic behavior of power system stability with simplicity in implementation.

References

[1] A. Ghasemi, H. Shayeghi, H. Alkhatib, Robust design of multimachine power system stabilizers using fuzzy gravitational search algorithm, International Journal of Electrical Power & Energy Systems 51 (2013) 190–200.

[2] H. Shayeghi, A. Ghasemi, Multiple pss design using an improved honey bee mating optimization algorithm to enhance low frequency oscillations, International Review of Electrical Engineering 6 (7).

[3] A. Khodabakhshian, M. J. Morshed, M. Parastegari, Coordinated design of statcom and excitation system controllers for multi-machine power systems using zero dynamics method, International Journal of Electrical Power & Energy Systems 49 (2013) 269–279.

[4] L.-Y. Sun, J. Zhao, G. M. Dimirovski, Adaptive coordinated passivation control for generator excitation and thyristor controlled series compensation system, Control Engineering Practice 17 (7) (2009) 766–772.

[5] L. Cong, Y. Wang, Co-ordinated control of generator excitation and statcom for rotor angle stability and voltage regulation enhancement of power systems, IEE Proceedings-Generation, Transmission and Distribution 149 (6) (2002) 659–666.

[6] N. Christl, Advanced series compensation with thyristor controlled impedance, CIGRE, 14/37/38-05.

[7] B. Agrawal, R. Hedin, R. Johnson, A. Montoya, B. Vossler, Advanced series compensation (asc) steady-state, transient stability, and subsynchronous resonance studies, in: Proceedings of Flexible AC Transmission Systems (FACTS) Conference, Boston, MA, 1992.

[8] R. Piwko, C. Wegner, S. Kinney, J. Eden, Subsynchronous resonance performance tests of the slatt thyristor-controlled series capacitor, IEEE Transactions on Power Delivery 11 (2) (1996) 1112–1119.

[9] H. Chen, Y. Wang, R. Zhou, Transient stability enhancement via coordinated excitation and upfc control, International journal of electrical power & energy systems 24 (1) (2002) 19–29.

[10] A. A. Hashmani, Y. Wang, T. Lie, Enhancement of power system transient stability using a nonlinear coordinated excitation and tcps controller, International journal of electrical power & energy systems 24 (3) (2002) 201–214.

[11] L. Cong, Y. Wang, D. Hill, Transient stability and voltage regulation enhancement via coordinated control of generator excitation and svc, International Journal of Electrical Power & Energy Systems 27 (2) (2005) 121–130.

[12] N. Mithulananthan, C. A. Canizares, J. Reeve, G. J. Rogers, Comparison of pss, svc, and statcom controllers for damping power system oscillations, IEEE transactions on power systems 18 (2) (2003) 786–792.

[13] L.-Y. Sun, J. Zhao, G. M. Dimirovski, Adaptive coordinated passivation control for generator excitation and thyristor controlled series compensation system, Control Engineering Practice 17 (7) (2009) 766–772.

[14] P. Pourbeik, M. J. Gibbard, Simultaneous coordination of power system stabilizers and facts device stabilizers in a multimachine power system for enhancing dynamic performance, IEEE Transactions on Power Systems 13 (2) (1998) 473–479.

[15] L.-J. Cai, I. Erlich, Simultaneous coordinated tuning of pss and facts damping controllers in large power systems, IEEE Transactions on Power Systems 20 (1) (2005) 294–300.

[16] Y. Abdel-Magid, M. Abido, Robust coordinated design of excitation and tcsc-based stabilizers using genetic algorithms, Electric Power Systems Research 69 (2-3) (2004) 129–141.

[17] X. Lei, E. N. Lerch, D. Povh, Optimization and coordination of damping controls for improving system dynamic performance, IEEE Transactions on Power Systems 16 (3) (2001) 473–480.

[18] H. Shayeghi, A. Safari, H. Shayanfar, Pss and tcsc damping controller coordinated design using pso in multi-machine power system, Energy Conversion and Management 51 (12) (2010) 2930–2937.

[19] M. Abido, Pole placement technique for pss and tcsc-based stabilizer design using simulated annealing, International journal of electrical power & energy systems 22 (8) (2000) 543–554.

[20] A. Khodabakhshian, R. Hooshmand, R. Sharifian, Power system stability enhancement by designing pss and svc parameters coordinately using rcga, in: Electrical and Computer Engineering, 2009. CCECE'09. Canadian Conference on, IEEE, 2009, pp. 579–582.

[21] S. Mishra, Neural-network-based adaptive upfc for improving transient stability performance of power system, IEEE Transactions on Neural Networks 17 (2) (2006) 461–470.

[22] Z. Min, L. Wei, Decentralized robust control for power systems with statcom, in: Electrical and Control Engineering (ICECE), 2010 International Conference on, IEEE, 2010, pp. 3520–3524.

[23] A. Ghasemi, A fuzzified multi objective interactive honey bee mating optimization for environmental/economic power dispatch with valve point effect, International Journal of Electrical Power & Energy Systems 49 (2013) 308–321.

[24] L. C. Saikia, N. Sinha, J. Nanda, Maiden application of bacterial foraging based fuzzy idd controller in agc of a multi-area hydrothermal system, International Journal of Electrical Power & Energy Systems 45 (1) (2013) 98–106.

[25] A. Abbadi, L. Nezli, D. Boukhetala, A nonlinear voltage controller based on interval type 2 fuzzy logic control system for multimachine power systems, International Journal of Electrical Power & Energy Systems 45 (1) (2013) 456–467.

[26] H. Shayeghi, A. Ghasemi, A multi objective vector evaluated improved honey bee mating optimization for optimal and robust design of power system stabilizers, International Journal of Electrical Power & Energy Systems 62 (2014) 630–645.

[27] C. A. Canizares, Power flow and transient stability models of facts controllers for voltage and angle stability studies, in: Power Engineering Society Winter Meeting, 2000. IEEE, Vol. 2, IEEE, 2000, pp. 1447–1454.

[28] S. Panda, N. Padhy, R. Patel, Modelling, simulation and optimal tun-

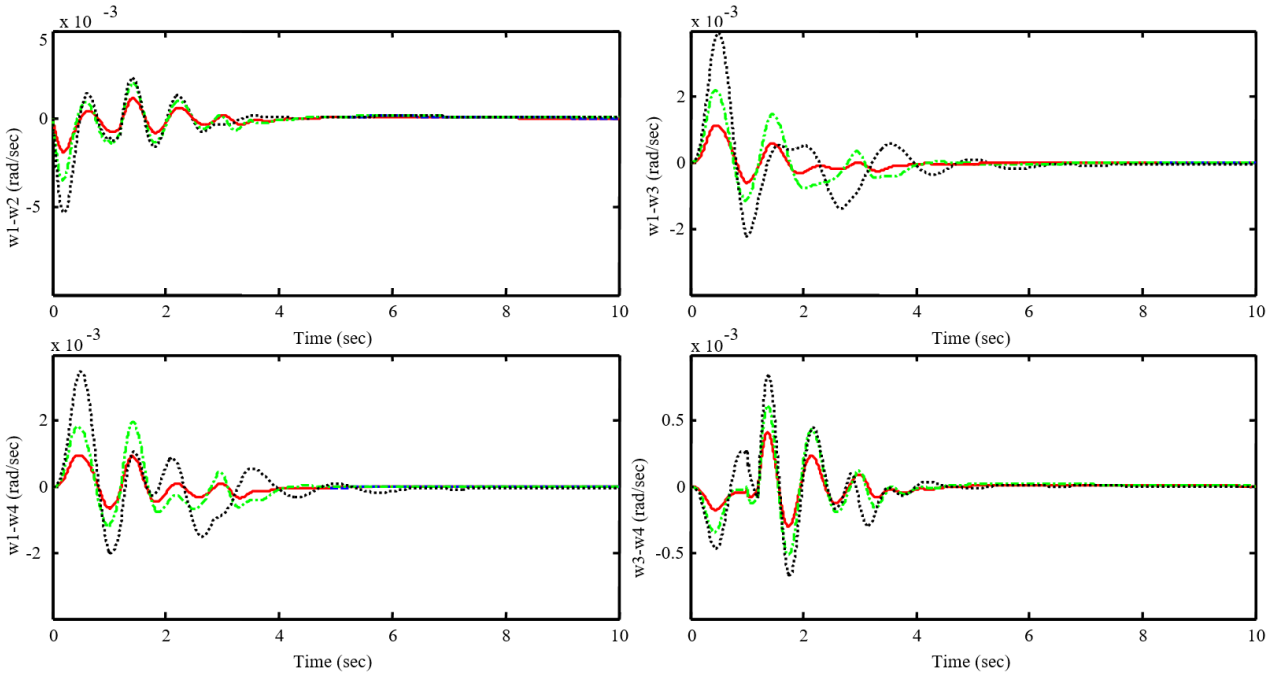

Figure 18: TAFM system response under nominal condition in scenario II; Solid (our Method) Dash-dotted (BFA [34]) and dot (CPSS [33])

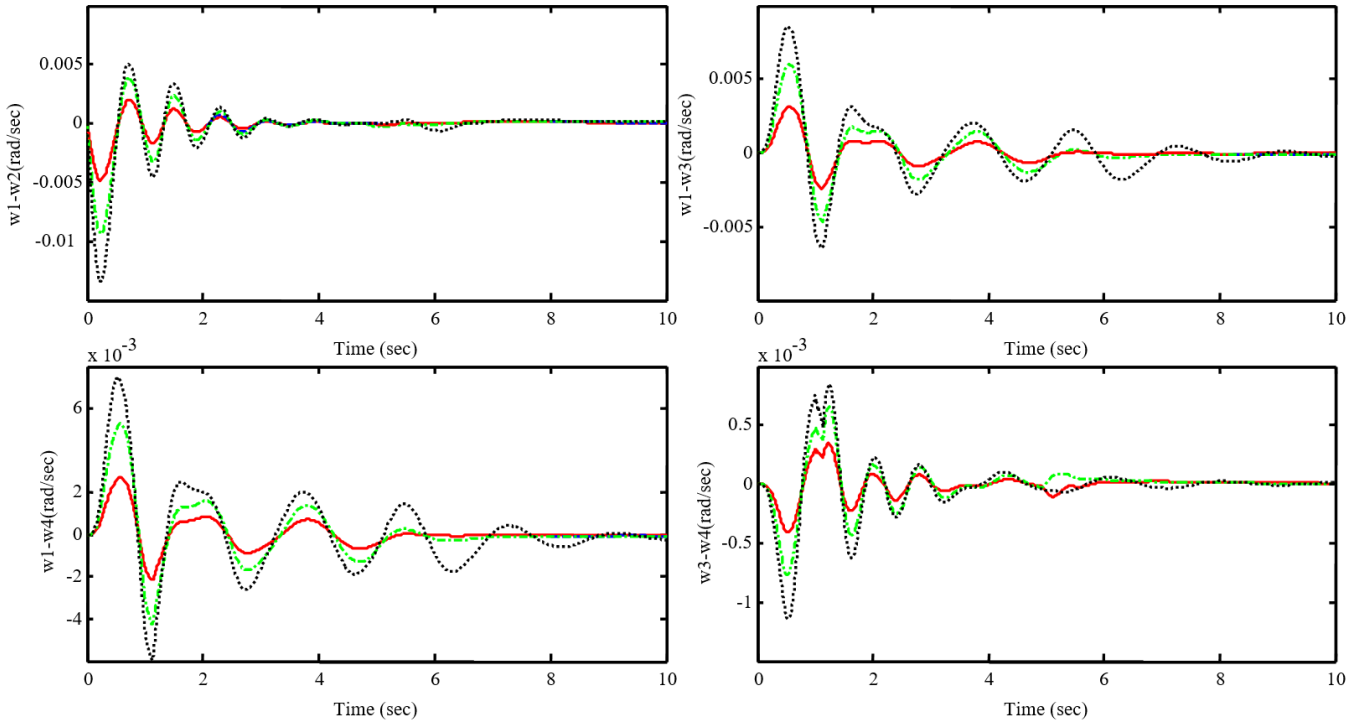

Figure 19: TAFM system response under night condition in scenario II; Solid (our Method) Dash-dotted (BFA [34]) and dot (CPSS [33])

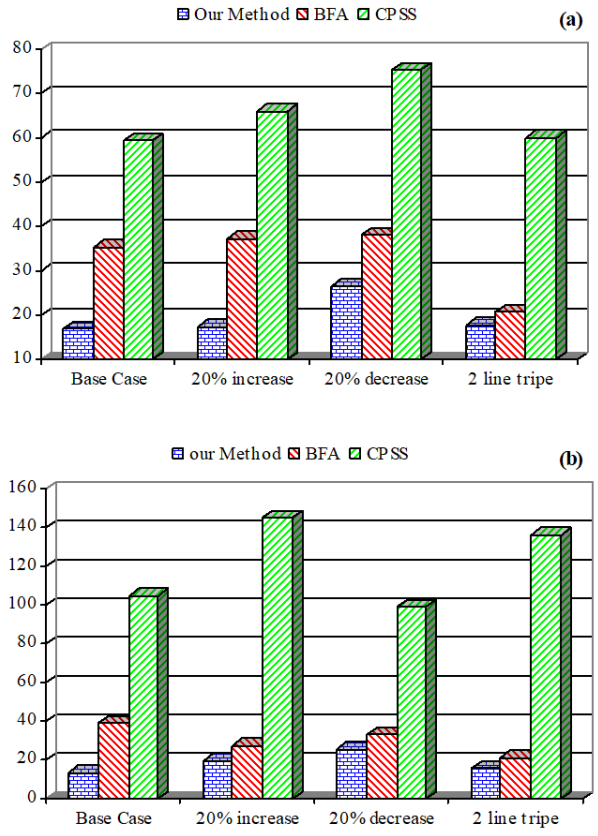

Figure 20: Values of performance index in scenario II; (a) ITAE and (b) FD

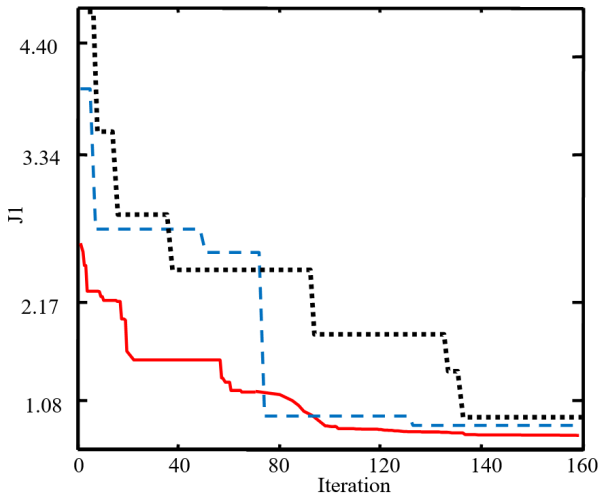

Figure 21: Fitness convergence with proposed algorithms; Solid (proposed Method), dashed (Tend) and dotted (logistic)

ing of tcsc controller., International Journal of Simulation Modelling (IJSIMM) 6 (1).

[29] C. Fuerte-Esquivel, E. Acha, H. Ambriz-Perez, A thyristor controlled series compensator model for the power flow solution of practical power networks, IEEE transactions on power systems 15 (1) (2000) 58–64.

[30] E. Rashedi, H. Nezamabadi-Pour, S. Saryazdi, Gsa: a gravitational search algorithm, Information sciences 179 (13) (2009) 2232–2248.

[31] D. Yang, G. Li, G. Cheng, On the efficiency of chaos optimization algorithms for global optimization, Chaos, Solitons & Fractals 34 (4) (2007) 1366–1375.

[32] H. Shayeghi, H. Shayanfar, A. Ghasemi, A robust abc based pss design for a smib power system, International Journal on Technical and Physical Problems of Engineering (IJTPE) 3 (2011) 86–92.

[33] K. Padiyar, Power system dynamics, BS publications, 2008.

[34] T. K. Das, G. K. Venayagamoorthy, U. O. Aliyu, Bio-inspired algorithms for the design of multiple optimal power system stabilizers: Sppso and bfa, IEEE Transactions on Industry Applications 44 (5) (2008) 1445–1457.

APPENDIX

4 machines System Data

Generator Data

Machine	1	2	3	4
H	55.575	55.575	58.5	58.5
Xd	0.2	0.2	0.2	0.2
$X'd$	0.033	0.033	0.033	0.033
Xq	0.19	0.19	0.19	0.19
$X'q$	0.016	0.016	0.016	0.016
Td'	8	8	8	8
Tq'	0.4	0.4	0.4	0.4
KA	200	200	200	200
TA	0.01	0.01	0.01	0.01
D	0	0	0	0

Line data

Line no.	From	To	R	X	B
1	1	5	0	0.0167	0
2	2	6	0	0.0167	0
3	3	8	0	0.0167	0
4	4	9	0	0.0167	0
5	5	6	0.0025	0.025	0.021875
6	8	9	0.0025	0.025	0.021875
7	6	7	0.001	0.01	0.00875
8	9	10	0.001	0.01	0.00875

Machine System bus data in per unit value

Bus no.	Type	Voltage	Angle	*Pload*	*Qload*	*Pgen*	*Qgen*
1	1	1.03	0	0	0	0	0
2	2	1.01	0	0	0	7	0
3	2	1.03	0	0	0	7	0
4	2	1.01	0	0	0	7	0
5	3	1	0	0	0	0	0
6	3	1	0	0	0	0	0
7	3	1	0	17.67	2.5	0	0
8	3	1	0	0	0	0	0
9	3	1	0	0	0	0	0
10	3	1	0	9.67	0	0	0